frontiers | Frontiers in Energy Research

TYPE Original Research
PUBLISHED 10 October 2024
DOI 10.3389/fenrg.2024.1372655

OPEN ACCESS

EDITED BY
Jiehao Wang,
Chevron, United States

REVIEWED BY
Pablo A. García-Salaberri,
Universidad Carlos III de Madrid, Spain
Liyuan Liu,
University of Science and Technology Beijing, China

*CORRESPONDENCE
Chaobin Guo,
guochaobin123@hotmail.com

RECEIVED 18 January 2024
ACCEPTED 10 May 2024
PUBLISHED 10 October 2024

CITATION
Guo C and Wang X (2024), Effect of permeability anisotropy on the CO_2 saturation distribution and phase change during a leakage event in a saline aquifer.
Front. Energy Res. 12:1372655.
doi: 10.3389/fenrg.2024.1372655

Effect of permeability anisotropy on the CO_2 saturation distribution and phase change during a leakage event in a saline aquifer

Chaobin Guo[1,2,3,4]* and Xinwen Wang[3,4,5]

[1]State Key Laboratory of Shale Oil and Gas Enrichment Mechanisms and Effective Development, Beijing, China, [2]SINOPEC Key Laboratory of Carbon Capture, Utilization and Storage, Beijing, China, [3]Chinese Academy of Geological Sciences, Beijing, China, [4]Technology Innovation Center for Carbon Sequestration and Geological Energy Storage, MNR, Beijing, China, [5]Petroleum Exploration and Development Research Institute, SINOPEC, Beijing, China

Predicting impacts of potential carbon dioxide (CO_2) leakage into shallow aquifers that overlie geologic CO_2 storage formations is an important part of developing reliable carbon storage technology. To quantifying the effect of permeability anisotropy, a three-dimensional hypothetical reservoir model was formulated to analyze the migration behavior of CO_2 under diverse permeability anisotropy scenarios. Sensitivity analyses for parameters corresponding to the permeability anisotropy and the leakage rate are conducted, and the results suggest that permeability anisotropy significantly affect the CO_2 migration characteristics. Increasing the parameter of vertical/horizontal permeability ratio results in longer CO_2 migration distances, which enhances the aqueous phase ratio and safety through more interaction with the aquifer, but also raises the potential of the leakage reaching the ground surface due to higher gas ratio. A comprehensive understanding of these dynamics is crucial for implementing effective monitoring and management strategies.

KEYWORDS

CO_2 geological storage, permeability anisotropy, numerical simulation, leakage evaluation, phase change

1 Introduction

Porous media brine-filled aquifers provide a substantial potential storage capacity for the geological carbon dioxide (CO_2) sequestration technology (Eccles et al., 2012; Karvounis and Blunt, 2021; Li et al., 2023a), which (Allen et al., 2018; Rycroft et al., 2024) is world widely considered a key element in addressing the climate crisis and achieving carbon neutrality goals (Celia et al., 2005). Assessing the negative environmental impact is a crucial aspect to ensure the long-term effective operation of the storage system using saline aquifers (Bradshaw et al., 2007; Navarre-sitchler et al., 2013). During the decision-making stage, a rational monitoring plan should be formulated by comprehensively considering geological features, groundwater flow, environmental impact, and so on (Miocic et al., 2019). This involves identifying the most likely areas for leakage and potential leakage pathways by considering the geological structure, permeability distribution, and groundwater flow paths in the underground formations. Therefore, specific simulations based on a thorough geological survey are necessary to determine the optimal monitoring positions

(Chadwick et al., 2008). Besides the monitoring locations, the monitoring frequency is also a key factor in a leakage assessment (Gunter et al., 2000; Romanak and Dixon, 2022).

The permeability anisotropy of underground formation implies the permeability differences between different directions. The permeability anisotropy directly affects the CO_2 migration paths as it flows through the formations, and in turn its distribution in the leakage assessment of the stored CO_2 underground (Bear and Corapcioglu, 1986; Ghanbari et al., 2006; Pei et al., 2024). For example, anisotropy may lead to an uneven distribution of CO_2 in underground rock formations, potentially forming asymmetric leakage paths (Dai et al., 2022; Pavan and Govindarajan, 2023). In formations like shales, where geological CO_2 storage might occur, the horizontal permeability can be notably higher than the vertical permeability (Liang et al., 2021; Sun et al., 2023; Gu et al., 2024). The laminar structure of shale facilitates fluid movement along the bedding planes, making understanding this anisotropic nature crucial in assessing the potential pathways for CO_2 migration and the associated risk of leakage. Conversely, in formations like sandstones with a more uniform and interconnected porosity, the ratio of horizontal to vertical permeabilities may be closer to 1, reflecting a more isotropic nature (Li et al., 2023b). The grains in sandstones create a network of pathways that allows CO_2 to traverse vertically with a similar ease as flow horizontally. This has implications for the potential transport of CO_2 and the risk of fluid migration to shallower aquifers or, in worst-case scenarios, to the surface. It points out that one needs to characterize permeability very carefully to reduce uncertainty in permeability, making predictions of CO_2 transport and monitoring plan more accurate and allowing for a more reliable optimization of operational choices (e.g., properties and density of wells, etc.) (Oldenburg et al., 2023).

However, despite some qualitative descriptions of the impact of permeability anisotropy on CO_2 migration, there is a lack of quantitative research on its effects (Zhang et al., 2017; Gan et al., 2021; Liu et al., 2021). It is worth noting the relatively limited number of ongoing storage projects, resulting in a shortage of on-site data for researching leakage incidents. For better prediction, prevention, and response to leakage incidents, it is essential to conduct in-depth research and draw upon existing lessons and experiences (Saleem et al., 2021; Mahjour and Faroughi, 2023). Simple theoretical analysis and analogies fall short in providing sufficient information for engineering applications under complex geological conditions. Therefore, it becomes important to conduct in-depth numerical simulations to analyze the effect of permeability anisotropy on CO_2 migration patterns, providing a more accurate and reliable guidance for future geological storage projects. Numerical simulations also need to consider anisotropy to model the migration of CO_2 in underground rock formations more realistically (Carrera and Neuman, 1986). While the numerical simulation method plays a critical role in the leakage assessment, it faces a series of challenges. These challenges mainly stem from the limited sample quantities and the use of approximate values for underground rock properties (Hortle et al., 2014; Wang et al., 2021; Legentil et al., 2023). As the number of samples from the underground formations is often limited, it is extremely challenging to fully characterize the geological structure and properties of these three-dimensional and highly anisotropic formations. This leads to the parameters and properties used in numerical simulations often being based on approximate values from the limited samples (Bianchi et al., 2016). The impact of this issue is primarily manifested in the uncertainty of simulation results. Numerical simulations cannot accurately reflect the real situation since the estimated range for anisotropy ratio spans from tens to hundreds, showcasing the substantial variability across different geological settings. Faced with this challenge, researchers need to better understand the reliability of simulation results by flexibly adjusting simulation parameters, employing sensitivity analysis, and pushing for innovation in geological exploration technologies to enhance the direct acquisition of underground rock properties (Nooraiepour, 2018).

Therefore, conducting an analysis of permeability anisotropy on leakage scenarios in geological CO_2 sequestration can assist researchers in better predicting potential leakage locations, leakage rates, and the non-uniformity of leakage paths. A three-dimensional hypothetical reservoir model was set up to analyze the migration behavior of CO_2 following its potential leakage into a saline aquifer under diverse permeability anisotropy scenarios. Through the numerical simulation examination of multiple permeability anisotropy configurations, this research could contribute insights essential to understanding and managing CO_2 sequestration and leakage risks in geological storage reservoirs, providing a good technical support for achieving carbon neutrality goals (Dai et al., 2022; Raats, 1973).

2 Materials and methods

2.1 Numerical methods

The CarbonFlow model was used as the simulation tool to do predictive modeling and sensitivity analyses of the fully coupled nonlinear equations describing mechanisms of CO_2 leakage. CarbonFlow is a module that has been derived from GPSFLOW (Cai et al., 2022), an general purpose subsurface flow simulator, which can model three-phase flow and transport over a wide range of pressures and temperatures encountered in reservoirs for water, CO_2 and NaCl. The governing equations and features related to permeability anisotropy and possible phase change of during CO_2 leakage to surface are listed following and other features can be found in the literature Cai et al. (2022), as shown in Table 1.

CarbonFlow uses the integral finite difference method of space discretization, which is the same in TOUGH3 (Jung et al., 2017). The permeability anisotropy could be characterized as $kx \neq ky \neq kz$ of each element. To keep descriptions simple, we assume that the permeabilities in the two directions on the horizontal plane are the same, which means $kx = ky$. Hence, the permeability anisotropy is represented by the ratio ($\alpha = kV/kH$), where kV is the vertical permeability and kH is the horizontal permeability.

During a leakage event, a change of phase composition (appearance or disappearance of a phase) might occur when certain parameters such as pressure and temperature exceed certain threshold values, like the critical point (Tcrit, Pcrit) = (31.04°C, 7.38 MPa) (Pruess, 2011), as shown in Figure 1. For example, the injected CO_2 at 1 km depth is normally in supcritical phase and will change to gas phase when migrating upward to 500 m depth. In CarbonFlow, three different fluid

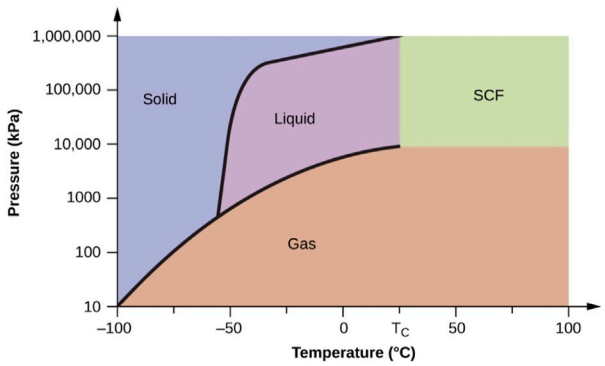

FIGURE 1
A phase diagram for carbon dioxide is shown. The pressure axis is plotted on a logarithmic scale to accommodate the large range of values (paul flowers et al., 2019).

phases may be present: an aqueous phase that is mostly water but may contain some dissolved CO_2, a liquid CO_2-rich phase that may contain some dissolved water, and a gaseous CO_2-rich that may contain some water. The fundamental thermodynamic properties are calculated based on the NIST database (Linstrom and Mallard, 2024).

2.2 Basic model design

2.2.1 Conceptual model and leakage rate

Potential pathways from saline formations have been detailed described in the IPCC's special report (Allen et al., 2018):1) through the pore system in low permeability caprocks if the capillary entry pressure is exceeded, 2) through opening in the caprock or fractures and faults, 3) through poorly completed and/or abandoned wells, and 4) through aquifers where dissolved CO_2 migrates laterally. It would be more than 100,000 years for CO_2 to leak through pore system in caprocks, and the flow in aquifers is estimated to be of the order of 1 mm/yr to 1 cm/yr.

As shown in Figure 2, this study focuses on leakage which can occur in just a few decades which operators can cope with and considers one simple scenario: leakage through faults or leakage through abandoned wells. Leakage through injection wells is excluded because these can be monitored relatively easily by operators and action can be taken when a leak occurs (Aoyagi et al., 2011). Leakage depth of 1,000 m is selected based on the depth description in Kalaydjian (Kalaydjian et al., 2011).

Since there is no sufficient on-site data research on leakage rate, and it depends on many factors including the geological conditions and operational conditions, 0.1% of annual storage mass is selected as the basic scenario based on the theoretical calculation considering natural carbon fluxes (Oldenburg et al., 2002). In the subsequent sensitivity analysis plan, the leakage rate is intended to be increased by 10 times to analyze this uncertainty factor. By increasing the leakage rate, the aim is to gain a deeper understanding of the system's response and stability in extreme scenarios, thereby accurately assessing potential risks. In this sturdy, we assume the stored CO_2 is 1 million tons per year, hence the leakage rate is 1,000 t/yr. The leakage continues 10 years, and we simulate to 20 years to study lateral migration characteristics.

2.2.2 Grids discretization

A three-dimensional hypothetical reservoir model was set up to analyze the migration behavior of CO_2 following its potential leakage into a saline aquifer under diverse permeability anisotropy scenarios. The mesh was created using mView software, which is a tool for mesh generation and management, as shown in Figure 3. The study area on the plane has been preliminarily chosen to be a 10 km by 10 km range based on prior research, which is larger than the affected area of the leak. Near the wellbore, at the center of the model, the mesh size is 2 m by 2 m. This finer grid extends to 50 m where the mesh size increases to 5 m by 5 m. Between 50 m and 5,000 m, the mesh size progressively increases with a multiplier of 2.5 starting from 5.0 m. There are a total of 1,521 cells in the horizontal plane. In the vertical direction, the mesh size near the leak point starts at 2 m and gradually increases to 20 m. Some grid refinements are conducted in the leakage and potential CO_2 phase change areas (from supercritical to

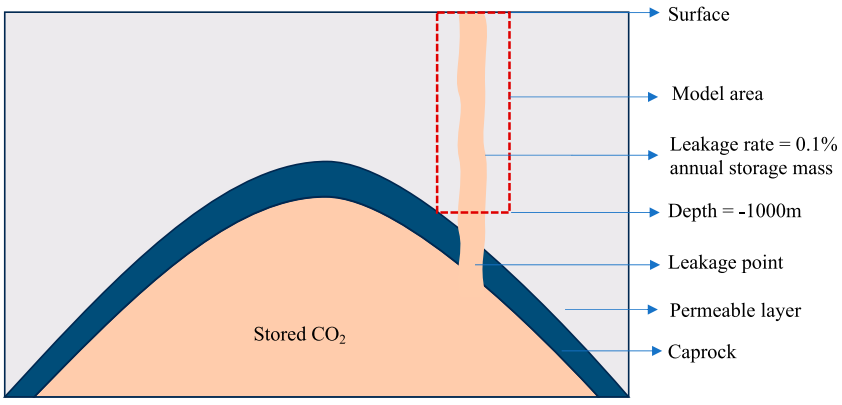

FIGURE 2
Conceptual model of CO_2 leakage in this study.

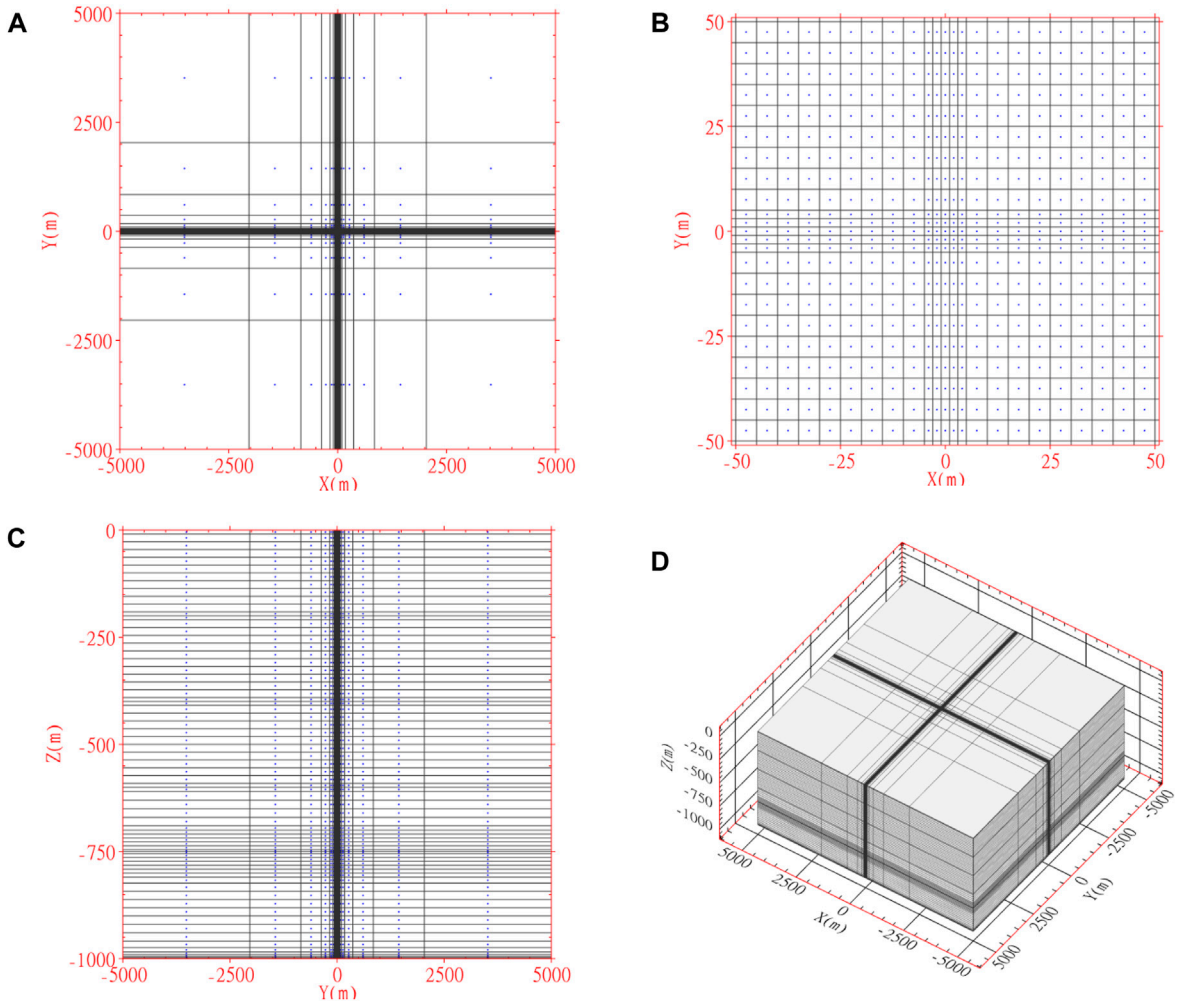

FIGURE 3
Domain discretization in plane perspective **(A)** with 1521 grids, grids refinement in the leakage area **(B)**, domain discretization in a vertical profile **(C)** by 69 layers with refinement in leakage layer and phase change area (700–800 m depth), and the entire 3D model with 104,949 grids **(D)**.

gas phases). There are 69 layers in total, comprising 104,949 cells overall.

2.2.3 Rock properties

We take the properties of Gudong Oilfield reservoir, which belongs to Shengli Oilfield, as a basic scenario in the hypothetical reservoir model. Data indicated porosity of 28%–35% in the Guantao Formation (Linye et al., 2004; Kalaydjian et al., 2011). Thus, an average porosity of 31% is determined to represent the sandstone in the basic model. The permeability of the sandstone is assumed to be 1,000 mD in the horizontal directions (kx = ky) as a basic scenario. This value is selected based on previous studies (evaluated permeability of 510-3118mD) and is considered a reasonable approximation in a typical horizontal reservoir. However, it's important to note that the actual permeability of the sandstone can vary depending on factors such as the depth of the reservoir, the pressure and temperature conditions, and the presence of fractures or other features that can affect fluid flow. Therefore, the permeability value used in the model should be considered as an approximation and would be adjusted in the next sensitivity studies. The other rock properties described in Kalaydjian (Kalaydjian et al., 2011) are used, as shown in Table 2.

The van Genuchten function (Van Genuchten, 1980) is used for the capillary pressure mode and the relative permeability mode, as in Pruess (Pruess et al., 1999). Hysteresis will certainly impact two-phase flow during the cycle of imbibition and drainage. But our focus is on the migration of CO_2 under constant leakage rate. Therefore, the hysteretic capillary pressure and relative permeability functions were not employed to account for a constant leakage rate since it was anticipated that the system would consistently remain on the drainage branch during the leakage phase, without undergoing repeated cycles of CO_2 leakage and water injection.

2.2.4 Initial and boundary conditions

Initially, the pressure is in a state of hydrostatic equilibrium, and the temperature is set according to a geothermal gradient of 0.03°C/

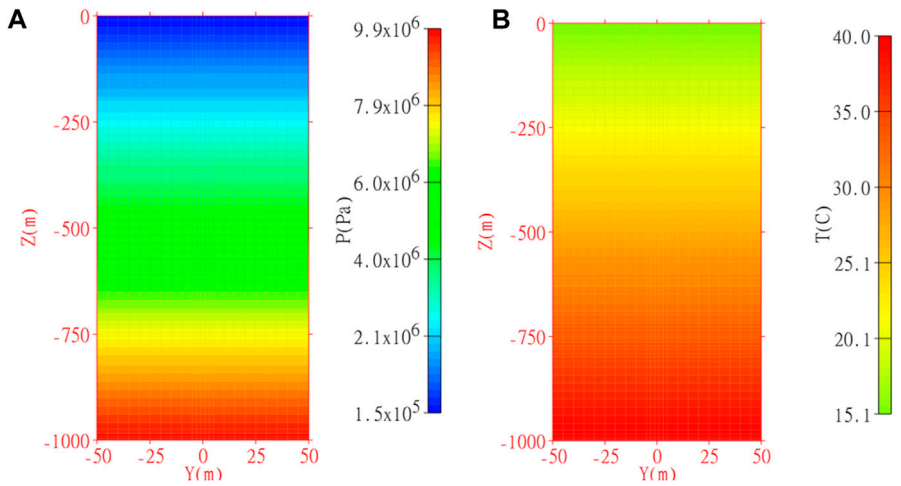

FIGURE 4
Initial pressure **(A)** and temperature **(B)** distribution.

TABLE 1 Governing equations used in CarbonFlow.

Parameter	Equations
Conservation of mass and energy	$\frac{d}{dt}\int_{V_n} M^i dV_n = \int_{\Gamma_n} F^i \cdot n d\Gamma_n + \int_{V_n} q^i dV_n$
Mass accumulation	$M^i = \Phi \sum_{\beta=1}^{NPH} S_\beta \rho_\beta X^i_\beta, i = 1, NK; \beta = 1, NPH$
Energy accumulation	$M^{NK+1} = \Phi \sum_{\beta=1}^{NPH} S_\beta \rho_\beta U_\beta + (1-\Phi)\rho_R C_R T$
Mass flux	$F^i = \sum_{\beta=1}^{NPH} X^i_\beta \rho_\beta u_\beta$
Energy flux	$F^{NK+1} = -\lambda \nabla T + \varphi \sum_{\beta=1}^{NPH} h_\beta \rho_\beta u_\beta$

V_n, an arbitrary subdomain bounded by the closed surface Γ_n; M^i, mass or energy accumulation term of component i per volume; F, mass or heat flux; n, normal vector on the surface element Γ_n pointing toward to V_n; q, sink/source term of mass or energy. Φ, porosity; β, phase index (e.g., β = gas, aqueous phase); S, saturation of phase β (the volume fractions of the pore space occupied by each phase); ρ_β, density of phase β; X^i_β, mass fraction of component i in phase β; NK, number of components; NPH, number of phases.

TABLE 2 Reservoir properties.

Property		Value	Unit
Density		2,640 Aoyagi et al. (2011)	kg/m^3
Porosity		0.31 Kalaydjian et al. (2011)	—
Permeability of horizontal direction		1.0×10^{-12}	m^2
Permeability of vertical direction		1.0×10^{-12}	m^2
Capillary pressure (P_c) and relative permeability (kr)	Exponent in expressions, m	0.40	—
	Irreducible water saturation, S_{lr}	0.20	—
	Irreducible gas saturation, S_{lr}	0.05	—
	Strength coefficient, P_0	3,584	Pa
	Maximum possible value of P_{cap}, P_{max}	1.0×10^7	Pa
	Saturated liquid phase, Sls	0.999	—

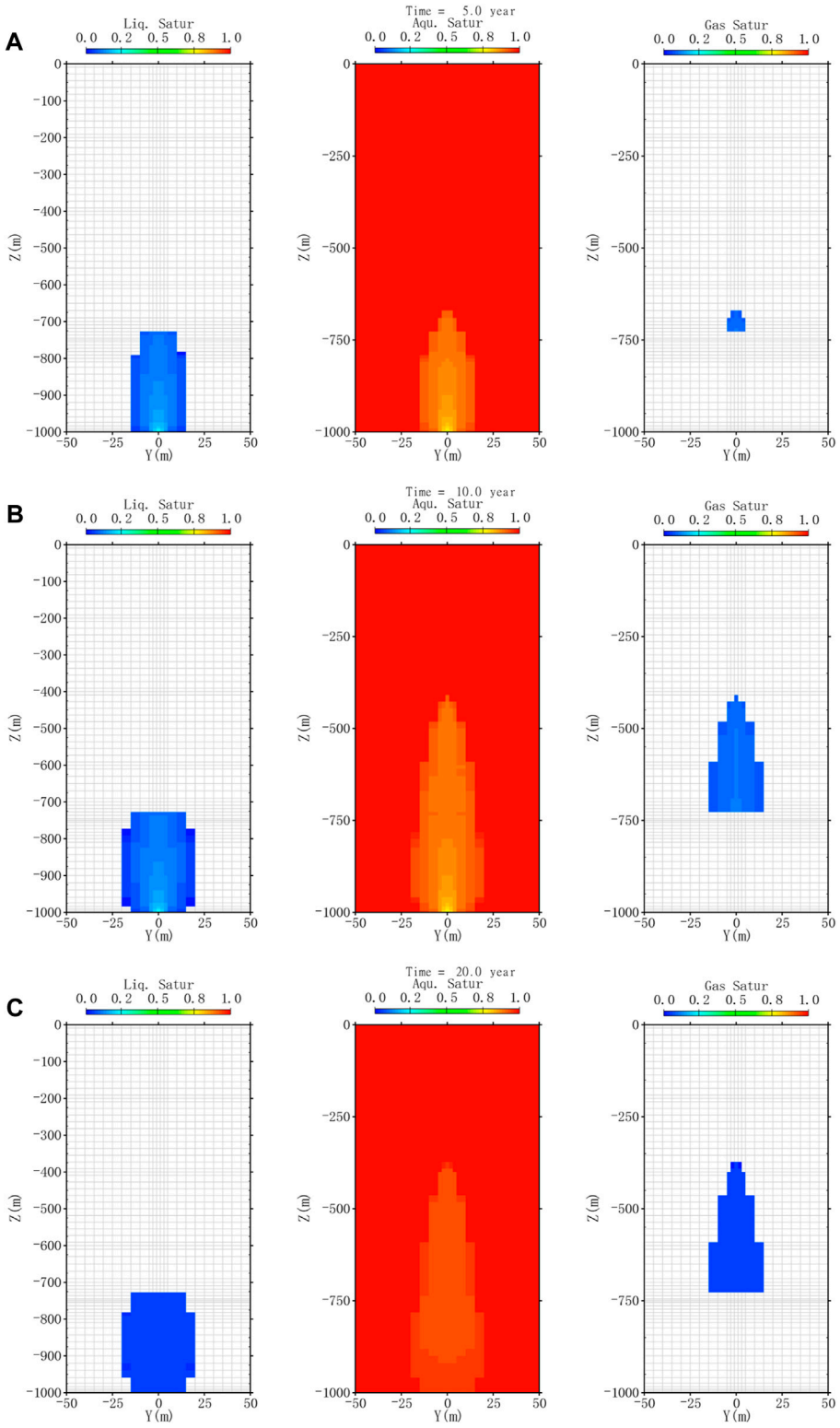

FIGURE 5
Phase saturation distribution and evolution on **(A)** 5-year, **(B)** 10-year and **(C)** 20-year.

m. The initial salinity of brine is 3% with no gas saturation, which has been used in the Aoyagi et al. (2011) and Wang et al. (2013). For visualization, we show initial conditions only for a portion of the domain (x = 0 m, y = −50 m–50 m, z = −1,000 m–0 m), because conditions are the same in the rest of the domain, as shown in Figure 4.

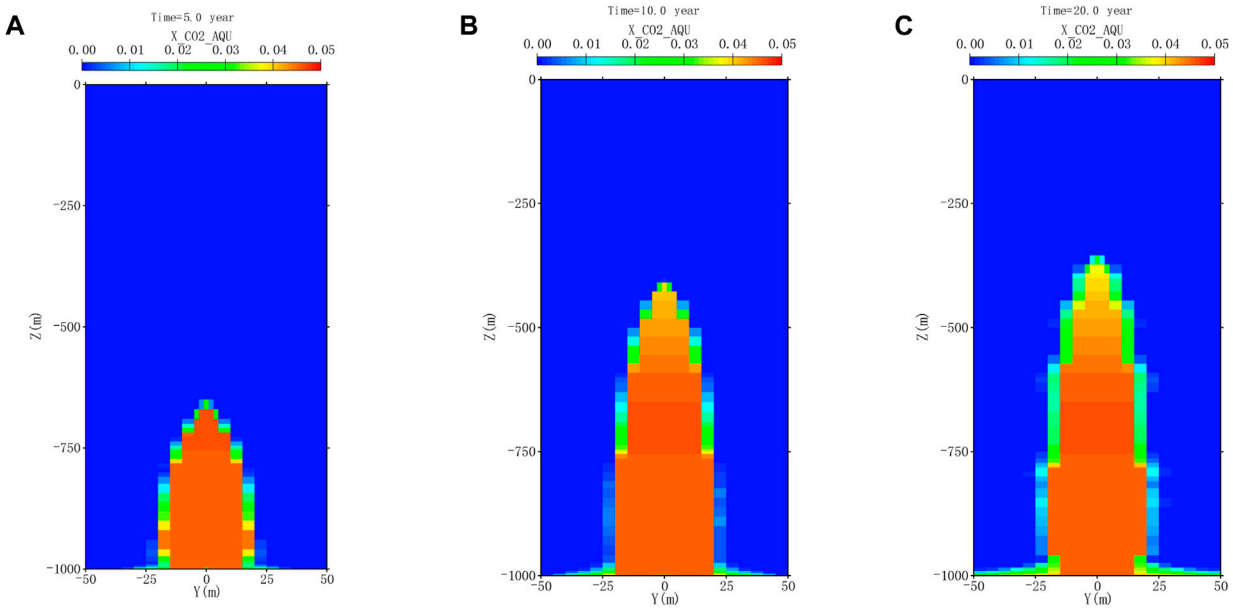

FIGURE 6
Mass fraction of CO_2 in aqueous phase distribution and evolution on **(A)** 5-year, **(B)** 10-year and **(C)** 20-year.

3 Results and discussion

3.1 CO_2 migration characterization

Figure 5 shows the phase saturation distribution and evolution. During the initial leakage period (0–5 years), as shown in Figure 5A, carbon dioxide primarily exists in the supercritical phase. Specifically, in our software, we categorize different phases using terms such as liquid phase, aqueous phase, and gas phase. Therefore, in the figure, we use the term "liquid phase" to represent the supercritical phase of carbon dioxide. From Figure 6A, in approximately the fifth year of the model, as it migrates upward to a depth of about 730 m, corresponding to the triple point conditions (pressure p = 7.38 MPa, temperature T = 31.04°C), CO_2 undergoes a significant transition from the liquid phase to the gas phase. This transformation plays a crucial role in the distribution and evolution of phase saturation within underground reservoirs. Changes in underground conditions lead to this shift in CO_2 state, thereby influencing the distribution of phase saturation.

As shown in Figure 5B, at the end of the leakage period (10th year), CO_2 migrates upward to a position at −400 m, covering an upward leakage distance of 600 m. Ten years after the leakage ceases, Figure 5C, a notable transformation occurs in the behavior of CO_2. During this period, the majority of CO_2 undergoes a phase transition, converting into the aqueous phase, as shown in Figure 6B. Despite the passage of time, the distance of its upward migration remains relatively unchanged at −360 m (Figure 6C). The relatively stable migration distance suggests that the dissolution process efficiently absorbs the leaked CO_2, preventing significant vertical movement. This phenomenon might be attributed to the limited quantity of leaked CO_2. The scarcity in leakage volume results in a predominant reliance on dissolution processes. Unlike scenarios with larger leaks, where gaseous CO_2 might travel greater distances due to buoyancy and pressure differentials, the modest volume of leaked CO_2 in this case allows dissolution to play a dominant role.

3.2 Permeability anisotropy

Various scenarios are designed as detailed in Table 3, where α ranges from 2^{-4} to 2 while the horizontal permeability remains constant. Ennis-king et al. (2005) conducted a study on how anisotropy affects the onset of instability, employing both linear and global stability analyses (Erfani et al., 2022). Their findings revealed that reducing α, while maintaining constant horizontal permeability and decreasing vertical permeability, stabilizes the process and impedes the initiation of instability. Due to the layered structure of natural formations, α is usually less than 1. In our design, we chose a maximum value of 2 to represent the broadest possible scenario. This design allows for realistic variations within the constraints of geological realities, providing a comprehensive exploration of permeability anisotropy.

3.2.1 CO_2 phase saturation distribution

Figures 7, 8 illustrate the distribution of phase saturation for various scenarios, offering a detailed glimpse into migration patterns over both 10 and 20 years. The analysis of figures shows a noticeable gathering of CO_2 around the leakage point at smaller scales. This is linked to a decrease in vertical permeability, constraining the paths for CO_2 migration and resulting in a significant reduction in movement within subsurface geological layers.

3.2.2 Trapping performance

In a storage unit, CO_2 in the aqueous phase is considered more stable than it in the gaseous or liquid phase. Therefore, we analyze

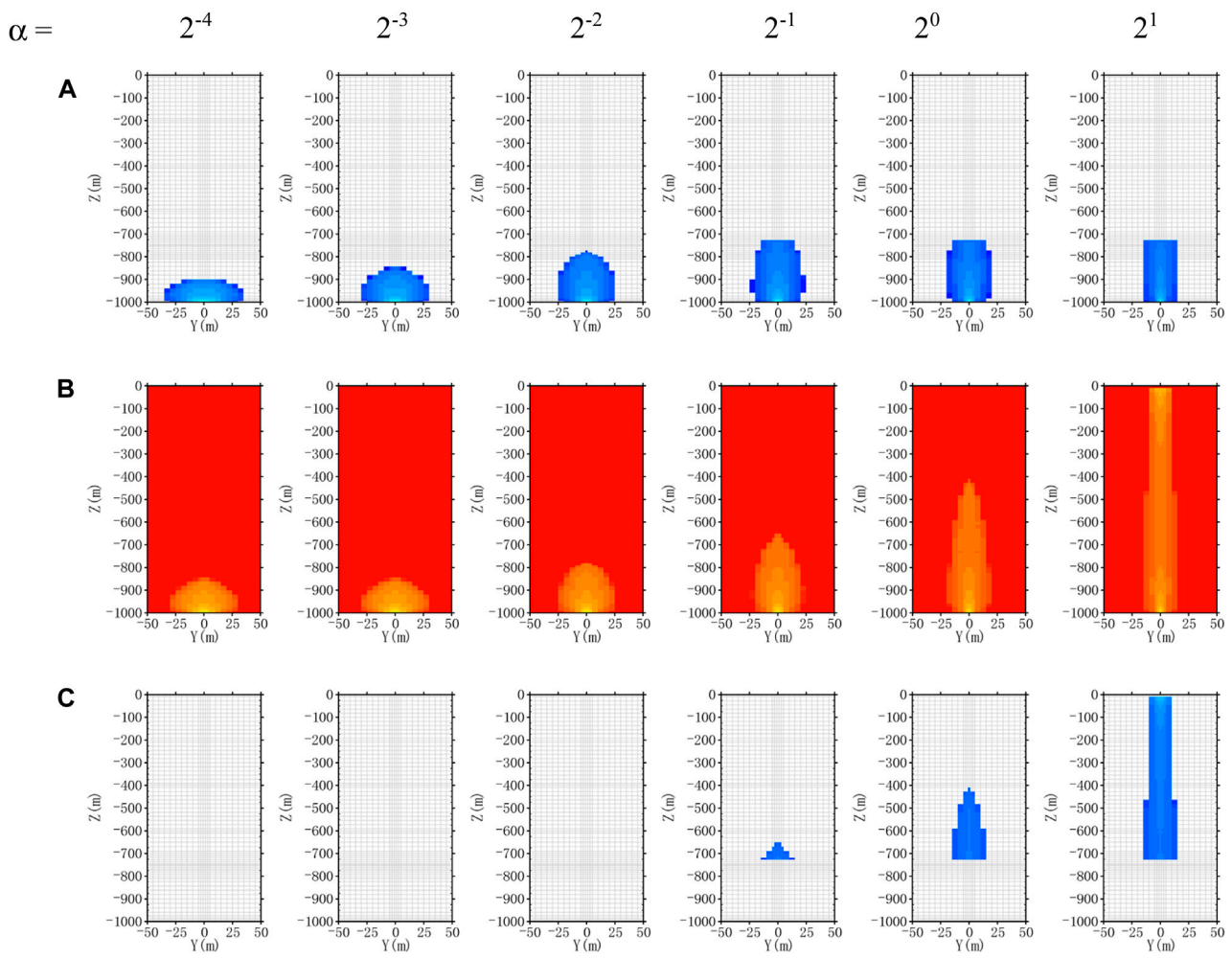

FIGURE 7
Phase saturation **(A)** Sl, **(B)** Sa and **(C)** Sg distribution of different α scenarios on 10-year.

CO_2 trapped in the aqueous phase for a more in-depth examination, aiming to understand the impact of permeability anisotropy, as shown in Figure 9.

At first glance, with an increase in the parameter α, CO_2 migration seems to move away from the leakage point, covering longer distances and encountering the aquifer more extensively. Consequently, the aqueous phase ratio becomes larger, suggesting a heightened level of safety in this context. This positive aspect is attributed to increased interaction with the aquifer, contributing to a more stable and secure scenario.

However, it is essential to note that the larger values of α also signify a higher gas ratio. This implies a greater proportion of the gas phase, characterized by increased mobility, which, in turn, raises the potential for leakage to the ground. Despite the advantageous aspect of a larger aqueous phase ratio, the elevated gas ratio introduces a concern related to the mobility of the CO_2, posing a risk of ground leakage.

Notably, when α equals 1, a critical threshold is reached. At this point, some CO_2 may migrate out of the ground, potentially causing damage to the surrounding environment. This emphasizes the delicate balance between safety and risk associated with varying values of α in the context of CO_2 migration. A comprehensive understanding of these dynamics is crucial for implementing effective monitoring and management strategies to ensure the safe storage and containment of CO_2, especially in scenarios where the parameter α reaches a critical value.

3.3 Leakage rate

The phase transitions and dissolution processes of CO_2 can vary with different leakage amounts. Two additional leakage rate scenarios (5 and 10 times the leakage rate in the basic model) were introduced to explore the interaction between leakage volume and permeability anisotropy.

The phase ratio for different leakage scenarios over 20 years, with α equal to 1.0, is illustrated in Figure 10. Despite the leakage rate increasing to 10 times that of the basic model, the phase ratio undergoes a relatively moderate change, reaching 40% of the leakage mass into the surface. Reducing α representing smaller vertical permeability, proves effective in preventing leakage to the surface, as indicated by the decreased leakage ratio in both Figures 11, 12.

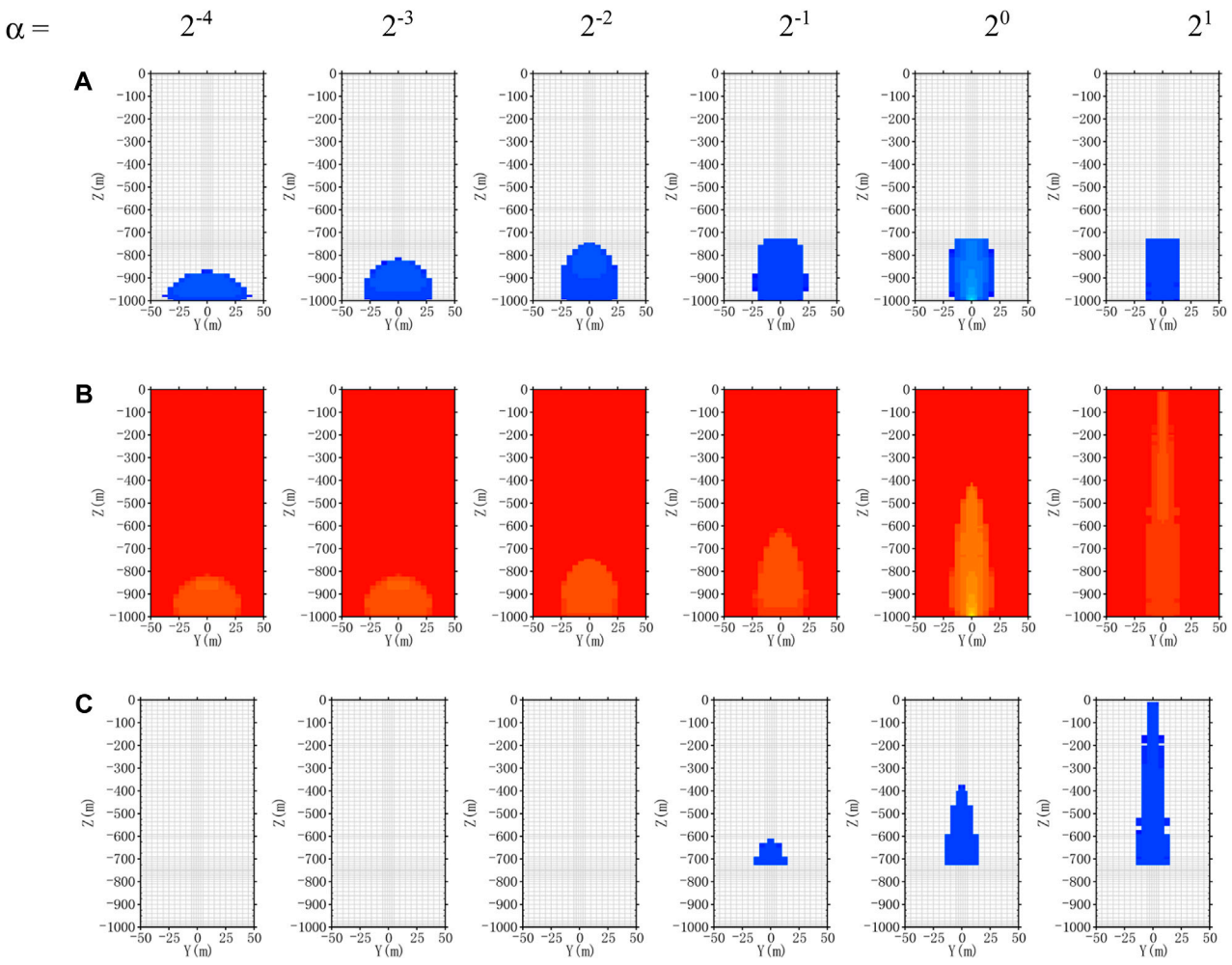

FIGURE 8
Phase saturation **(A)** Sl, **(B)** Sa and **(C)** Sg distribution of different α scenarios on 20-year.

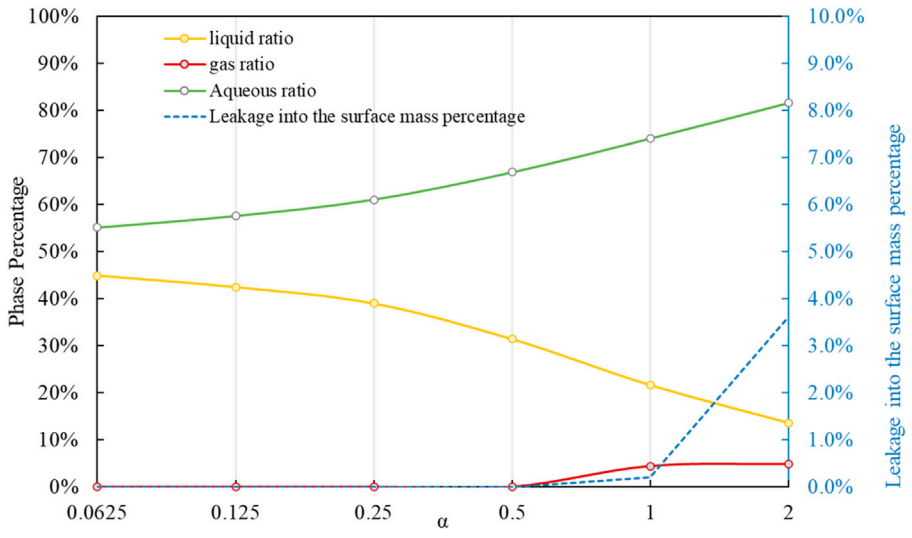

FIGURE 9
Phase ration of different α scenarios on 20-year.

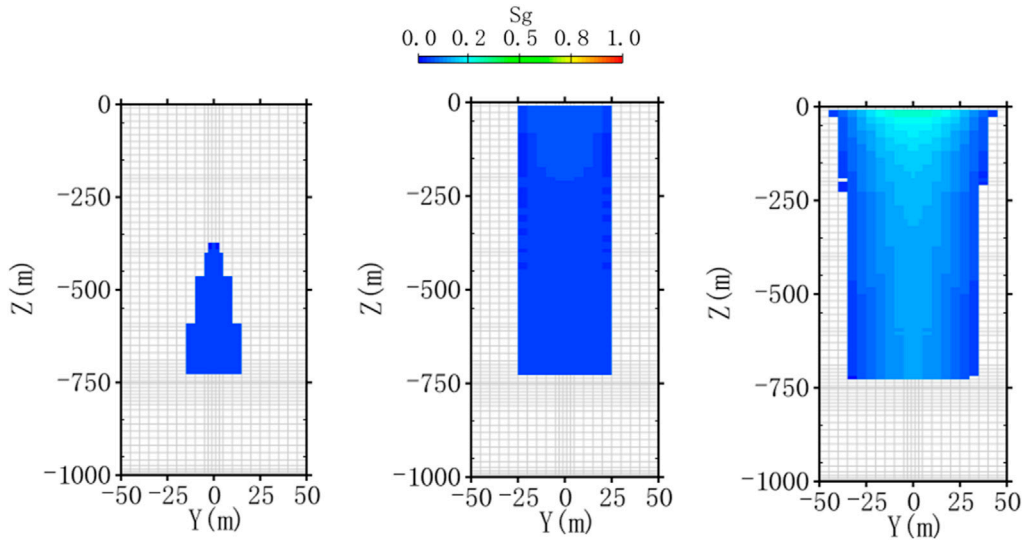

FIGURE 10
Gas phase saturation distribution of different leakage rate scenarios (from left to right refer to 0.1%, 0.5%, 1.0%) at 20 years (α = 1.0).

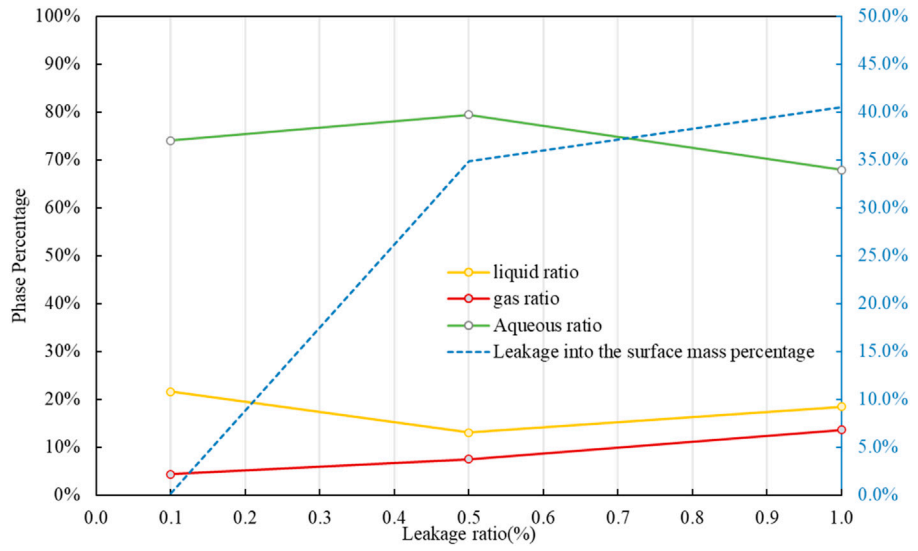

FIGURE 11
Phase partitions of different leakage ratio scenarios at 20 years (α = 1.0).

TABLE 3 Scenarios design of permeability anisotropy.

Parameter	Value	Note (m^2)
α	2^{-4}, 2^{-3}, 2^{-2}, 2^{-1}, 2^{0}, 2^{1}	kH = 1.0 × 10^{-12}

4 Conclusion

A comprehensive three-dimensional reservoir model was set up to analyze the migration behavior of CO_2 under diverse permeability anisotropy scenarios. The investigation demonstrated that the complex interaction of permeability anisotropy, manifesting as varied permeability values in horizontal and vertical directions within the rock structure, can substantially modify the spread of CO_2 both horizontally and vertically. Sensitivity analyses indicated that the response of the reservoir to changes in permeability anisotropy is not uniform, suggesting that a one-size-fits-all approach to site evaluation may be inadequate. Instead, the simulation outcomes underscore the necessity for tailored acceptance criteria that reflect the unique properties and operational parameters of individual storage sites. Consequently, these

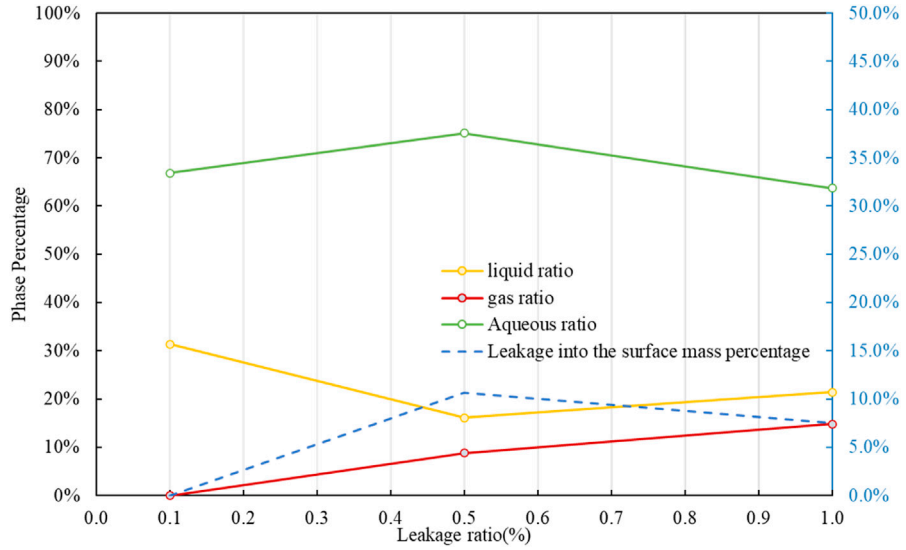

FIGURE 12
Phase partitions of different leakage ratio scenarios on 20-year (α = 0.5).

results provide a robust framework for the assessment and design of potential storage sites, enabling a more precise estimation of the risks associated with CO_2 leakage.

In practice, the variability in these ratios across different geological settings highlights the need for detailed site-specific investigations to enhance our understanding of subsurface processes related to CO_2 storage. Hence, a thorough consideration of the impact of permeability anisotropy on the assessment of CO_2 geological sequestration leakage is crucial. Advances in technology and comprehensive data collection methods continue to contribute to refining our knowledge of rock permeability, ultimately supporting sustainable and informed decision-making in geological carbon dioxide storage.

Data availability statement

The original contributions presented in the study are included in the article/Supplementary material, further inquiries can be directed to the corresponding author.

Author contributions

CG: Writing–original draft, Writing–review and editing. XW: Conceptualization, Methodology, Software, Writing–original draft.

Funding

The author(s) declare that financial support was received for the research, authorship, and/or publication of this article. Financially supported by the Open Fund of SINOPEC Key Laboratory of Carbon Capture, Utilization and Storage, National Natural Science Foundation of China (42372286, U2244215, and U2344226), Chinese Geological Survey Projects (DD20221819), and the Basic Research Fund of the Chinese Academy of Geological Sciences (JKYQN202306).

Conflict of interest

Author XW was employed by Petroleum Exploration and Development Research Institute, SINOPEC.

CG is a member of SINOPEC Key Laboratory of Carbon Capture, Utilization and Storage and Petroleum Exploration and Development Research Institute, SINOPEC.

Publisher's note

References

Allen, M., Dube, O., Solecki, W., et al. (2018) *Special report: global warming of 1.5 C.* China: Intergovernmental Panel on Climate Change IPCC.

Aoyagi, R., Kitamura, O., Itaoka, K., Igawa, S., and Suzuki, S. (2011). Study on role of simulation of possible leakage from geological CO2 storage in sub-seabed for environmental impact assessment. *Energy Procedia* 4, 3881–3888. doi:10.1016/j.egypro.2011.02.325

Bear, J., and Corapcioglu, M. Y. (1986). Transport phenomena in porous media. *Eos, Trans. Am. Geophys. Union* 67, 92–93. doi:10.1029/eo067i008p00092-06

Bianchi, M., Zheng, L., and Birkholzer, J. T. (2016). Combining multiple lower-fidelity models for emulating complex model responses for CCS environmental risk assessment. *Int. J. Greenh. Gas Control* 46, 248–258. doi:10.1016/j.ijggc.2016.01.009

Bradshaw, J., Bachu, S., Bonijoly, D., Burruss, R., Holloway, S., Christensen, N. P., et al. CO2 storage capacity estimation: issues and development of standards. , 2007, 1(1): 62–68. doi:10.1016/s1750-5836(07)00027-8

Cai, Z., Zhang, K., and Guo, C. (2022). Development of a novel simulator for modelling underground hydrogen and gas mixture storage. *Int. J. Hydrogen Energy* 47 (14), 8929–8942. doi:10.1016/j.ijhydene.2021.12.224

Carrera, J., and Neuman, S. P. (1986). Estimation of aquifer parameters under transient and steady state conditions: 1. Maximum likelihood method incorporating prior information. *Water Resour. Res.* 22 (2), 199–210. doi:10.1029/wr022i002p00199

Celia, M., States, U., Canada, B. G., et al. (2005) *Underground geological storage*.

Chadwick, A., Arts, R., Bernstone, C., May, F., Thibeau, S., and Zweigel, P. (2008). *Best practice for the storage of CO_2 in saline aquifers—observations and guidelines from the SACS and CO_2STORE projects*. Available at: https://nora.nerc.ac.uk/id/eprint/2959.

Dai, S.-X., Dong, Y.-J., Wang, F., Xing, Z. h., Hu, P., and Yang, F. (2022). A sensitivity analysis of factors affecting in geologic CO2 storage in the Ordos Basin and its contribution to carbon neutrality. *China Geol.* 5 (3), 1–13. doi:10.31035/cg2022019

Eccles, J. K., Pratson, L., Newell, R. G., and Jackson, R. B. (2012). The impact of geologic variability on capacity and cost estimates for storing CO2 in deep-saline aquifers. *Energy Econ.* 34 (5), 1569–1579. doi:10.1016/j.eneco.2011.11.015

Ennis-King, J., Preston, I., and Paterson, L. (2005). Onset of convection in anisotropic porous media subject to a rapid change in boundary conditions. *Phys. Fluids* 17 (8), 084107. doi:10.1063/1.2033911

Erfani, H., Babaei, M., Berg, C. F., and Niasar, V. (2022). Scaling CO2 convection in confined aquifers: effects of dispersion, permeability anisotropy and geochemistry. *Adv. Water Resour.* 164, 104191. doi:10.1016/j.advwatres.2022.104191

Gan, M., Nguyen, M. C., Zhang, L., Wei, N., Li, J., Lei, H., et al. (2021). Impact of reservoir parameters and wellbore permeability uncertainties on CO2 and brine leakage potential at the Shenhua CO2 Storage Site, China. *Int. J. Greenh. Gas Control* 111, 103443. doi:10.1016/j.ijggc.2021.103443

Ghanbari, S., al-Zaabi, Y., Pickup, G. E., Mackay, E., Gozalpour, F., and Todd, A. (2006). Simulation of CO2 storage in saline aquifers. *Chem. Eng. Res. Des.* 84 (9), 764–775. doi:10.1205/cherd06007

Gu, M.-Z., Sheng, M., Zhuang, X.-Y., Li, X. Y., and Li, G. S. (2024). The influences of perforating phase and bedding planes on the fracture deflection in laminated shale. *Petroleum Sci.* 21 (2), 1221–1230. doi:10.1016/j.petsci.2023.10.015

Gunter, W. D., Perkins, E. H., and Hutcheon, I. (2000). Aquifer disposal of acid gases: modelling of water–rock reactions for trapping of acid wastes. *Appl. Geochem.* 15 (8), 1085–1095. doi:10.1016/s0883-2927(99)00111-0

Hortle, A., Michael, K., and Azizi, E. (2014). Assessment of CO2 storage capacity and injectivity in saline aquifers – comparison of results from numerical flow simulations, analytical and generic models. *Energy Procedia* 63, 3553–3562. doi:10.1016/j.egypro.2014.11.384

Jung, Y., Pau, G. S. H., Finsterle, S., and Pollyea, R. M. (2017). TOUGH3: a new efficient version of the TOUGH suite of multiphase flow and transport simulators. *Comput. Geosciences* 108, 2–7. doi:10.1016/j.cageo.2016.09.009

Kalaydjian, F., Zhang, J., Broutin, P., Hetland, J., Xu, S., Poulsen, N. E., et al. (2011). Preparing the ground for the implementation of a large-scale CCS demonstration in China based on an IGCC-CCS thermal power plant: the China-EU COACH Project. *Energy Procedia* 4, 6021–6028. doi:10.1016/j.egypro.2011.02.606

Karvounis, P., and Blunt, M. J. (2021). Assessment of CO2 geological storage capacity of saline aquifers under the North Sea. *Int. J. Greenh. Gas Control* 111, 103463. doi:10.1016/j.ijggc.2021.103463

Legentil, C., Pellerin, J., Raguenel, M., and Caumon, G. (2023). Towards a workflow to evaluate geological layering uncertainty on CO2 injection simulation. *Appl. Comput. Geosciences* 18, 100118. doi:10.1016/j.acags.2023.100118

Liang, M., Wang, Z., Zhang, Y., Greenwell, C. H., Li, H., Yu, Y., et al. (2021). Experimental investigation on gas permeability in bedding shale with brittle and semi-brittle deformations under triaxial compression. *J. Petroleum Sci. Eng.* 196, 108049. doi:10.1016/j.petrol.2020.108049

Linstrom, P. J., and Mallard, W. G. (2024). NIST chemistry WebBook, NIST standard reference database number 69. Gaithersburg MD. *J. Chem. Eng. Data*, 20899.

Linye, Z., Shouchun, Z., Zhilin, C., Chunrong, Z., and Zhihua, H. (2004). THE GENERATION OF IMMATURE OILS IN THE LACUSTRINE JIYANG MEGA-DEPRESSION, BOHAI BAY BASIN, CHINA. *J. Petroleum Geol.* 27 (4), 389–402. doi:10.1111/j.1747-5457.2004.tb00065.x

Liu, J., Xie, L., He, B., Gan, Q., and Zhao, P. (2021). Influence of anisotropic and heterogeneous permeability coupled with *in-situ* stress on CO2 sequestration with simultaneous enhanced gas recovery in shale: quantitative modeling and case study. *Int. J. Greenh. Gas Control* 104, 103208. doi:10.1016/j.ijggc.2020.103208

Li, X., Duan, K., Zhang, Q., Li, J., Jiang, R., and Wang, L. (2023b). Investigation of the permeability anisotropy of porous sandstone induced by complex stress conditions. *Comput. Geotechnics* 157, 105309. doi:10.1016/j.compgeo.2023.105309

Li, Y., Wang, R., Zhao, Q., Xue, Z., and Zhou, Y. (2023a). A CO2 storage potential evaluation method for saline aquifers in a petroliferous basin. *Petroleum Explor. Dev.* 50 (2), 484–491. doi:10.1016/s1876-3804(23)60403-3

Mahjour, S. K., and Faroughi, S. A. (2023). Risks and uncertainties in carbon capture, transport, and storage projects: a comprehensive review. *Gas Sci. Eng.* 119, 205117. doi:10.1016/j.jgsce.2023.205117

Miocic, J. M., Gilfillan, S. M. V., Frank, N., Schroeder-Ritzrau, A., Burnside, N. M., and Haszeldine, R. S. (2019). 420,000 year assessment of fault leakage rates shows geological carbon storage is secure. *Sci. Rep.* 9 (1), 769. doi:10.1038/s41598-018-36974-0

Navarre-Sitchler, A. K., Maxwell, R. M., Siirila, E. R., Hammond, G. E., and Lichtner, P. C. (2013). Elucidating geochemical response of shallow heterogeneous aquifers to CO2 leakage using high-performance computing: implications for monitoring of CO2 sequestration. *Adv. Water Resour.* 53, 45–55. doi:10.1016/j.advwatres.2012.10.005

Nooraiepour, M. (2018) *Rock properties and sealing efficiency in fine-grained siliciclastic caprocks — implications for CCS and petroleum industry*.

Oldenburg, C. M., Finsterle, S., and Trautz, R. C. (2023). Water upconing in underground hydrogen storage: sensitivity analysis to inform design of withdrawal. *Transp. Porous Media* 151, 55–84. doi:10.1007/s11242-023-02033-0

Oldenburg, C. M., Unger, A. J. A., Hepple, R. P., et al. (2002) *On leakage and seepage from geological carbon sequestration sites*.

Paul Flowers, K. T., Langley, RICHARD, William, R., and Robinson, P. H. D. (2019) *Chemistry 2e. OpenStax*.

Pavan, T. N. V., and Govindarajan, S. K. (2023). Numerical investigations on performance of sc-CO2 sequestration associated with the evolution of porosity and permeability in low permeable saline aquifers. *Geoenergy Sci. Eng.* 225, 211681. doi:10.1016/j.geoen.2023.211681

Pei, X., Liu, Y., Lin, Z., Fan, P., Mi, L., and Xue, L. (2024). Anisotropic dynamic permeability model for porous media. *Petroleum Explor. Dev.* 51 (1), 193–202. doi:10.1016/s1876-3804(24)60016-9

Pruess, K. (2011) *ECO2M: a TOUGH2 fluid property module for mixtures of water, NaCl, and CO2, including super- and sub-critical conditions, and phase change between liquid and gaseous CO2.*

Pruess, K., Oldenburg, C. M., and Moridis, G. J. (1999) *TOUGH2 user's guide version 2*.

Raats, P. A. C. (1973) *Dynamics of fluids in porous media*. America: Soil Science Society of America Journal.

Romanak, K., and Dixon, T. (2022). CO2 storage guidelines and the science of monitoring: achieving project success under the California Low Carbon Fuel Standard CCS Protocol and other global regulations. *Int. J. Greenh. Gas Control* 113, 103523. doi:10.1016/j.ijggc.2021.103523

Rycroft, L., Neele, F., and Monea, M. (2024) *Chapter one - introduction to carbon capture and storage [M]//RYCROFT L, NEELE F. Deployment of carbon capture and storage*. USA: Woodhead Publishing, 1–23.

Saleem, U., Dewar, M., Chaudhary, T. N., Sana, M., Lichtschlag, A., Alendal, G., et al. (2021). Numerical modelling of CO2 migration in heterogeneous sediments and leakage scenario for STEMM-CCS field experiments. *Int. J. Greenh. Gas Control* 109, 103339. doi:10.1016/j.ijggc.2021.103339

Sun, C., Nie, H., Su, H., Du, W., Lu, T., Chen, Y., et al. (2023). Porosity, permeability and rock mechanics of Lower Silurian Longmaxi Formation deep shale under temperature-pressure coupling in the Sichuan Basin, SW China. *Petroleum Explor. Dev.* 50 (1), 85–98. doi:10.1016/s1876-3804(22)60371-9

van Genuchten, M. (1980). A closed-form equation for predicting the hydraulic conductivity of unsaturated soils. *Soil Sci. Soc. Am. J.* 44, 892–898. doi:10.2136/sssaj1980.03615995004400050002x

Wang, F., Ping, S., Yuan, Y., Sun, Z., Tian, H., and Yang, Z. (2021). Effects of the mechanical response of low-permeability sandstone reservoirs on CO2 geological storage based on laboratory experiments and numerical simulations. *Sci. Total Environ.* 796, 149066. doi:10.1016/j.scitotenv.2021.149066

Wang, Y., Zhang, K., and Wu, N. (2013). Numerical investigation of the storage efficiency factor for CO2 geological sequestration in saline formations. *Energy Procedia* 37, 5267–5274. doi:10.1016/j.egypro.2013.06.443

Zhang, G., Lu, P., Ji, X., and Zhu, C. (2017). CO2 plume migration and fate at sleipner, Norway: calibration of numerical models, uncertainty analysis, and reactive transport modelling of CO2 trapping to 10,000 years. *Energy Procedia* 114, 2880–2895. doi:10.1016/j.egypro.2017.03.1410